Electronic Supplementary Information

Differentiating ion transport of water-in-salt electrolytes within micro- and mesopores of a multiporous carbon electrode

M. Tauhidul Islam[1], Bernhard Gollas[1], Qamar Abbas[1,2,*]

Institute for Chemistry and Technology of Materials, Graz University of Technology, Stremayrgasse 9, 8010 Graz, Austria

Institute of Chemistry and Technical Electrochemistry, Poznan University of Technology, Berdychowo 4, 60965 Poznan, Poland

[*]Corresponding author email: qamar.abbas@tugraz.at

Table of contents

Table S1: Salt to water volume ratio, salt to water weight ratio and water to salt molar mass ratio for different concentration of electrolytes prepared from ChCl and LiTFSI.

Salt type	Molal concen-ration (mol·kg^{-1})	Mass of water (g)	Mass of salt (g)	Volume of water (cm^3) (density 1.004 g·cm^{-3} at 25 °C)	Volume of salt (cm^3) (density 1.1 g/cm^3 at 25 °C)	Salt to water volume ratio	Salt to water weight ratio	Moles of water	Moles of salt	Water to salt molar ratio
ChCl	0.1	10	0.139	9.96	0.13	0.01	0.01	0.56	0.001	557.57
	0.5	10	0.695	9.96	0.63	0.06	0.07	0.56	0.005	111.51
	1	10	1.39	9.96	1.26	0.13	0.14	0.56	0.01	55.76
	2	10	2.78	9.96	2.53	0.25	0.28	0.56	0.02	27.88
	5	10	6.95	9.96	6.32	0.63	0.70	0.56	0.05	11.15
	10	10	13.9	9.96	12.64	1.27	1.39	0.56	0.10	5.58
	15	10	20.85	9.96	18.95	1.90	2.09	0.56	0.15	3.72
	20	10	27.8	9.96	25.27	2.54	2.78	0.56	0.20	2.79
	25	10	34.75	9.96	31.59	3.17	3.48	0.56	0.25	2.23
LiTFSI	0.1	10	0.287	9.96	0.22	0.02	0.03	0.56	0.001	555.29
	0.5	10	1.44	9.96	1.08	0.11	0.14	0.56	0.005	110.67
	1	10	2.87	9.96	2.16	0.22	0.29	0.56	0.01	55.53
	2	10	5.74	9.96	4.32	0.43	0.57	0.56	0.02	27.76
	5	10	14.35	9.96	10.79	1.08	1.44	0.56	0.05	11.10
	10	10	28.71	9.96	21.59	2.17	2.87	0.56	0.10	5.55
	15	10	43.07	9.96	32.38	3.25	4.31	0.56	0.15	3.70
	20	10	57.42	9.96	43.17	4.33	5.74	0.56	0.20	2.78

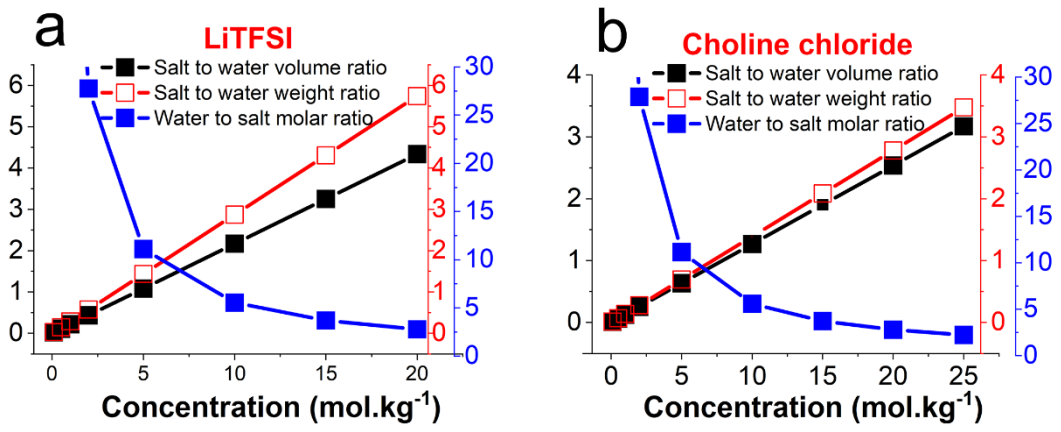

Figure S1: Salt to water volume ratio, salt to water weight ratio and water to salt molar ratio for a) LiTFSI and b) ChCl.

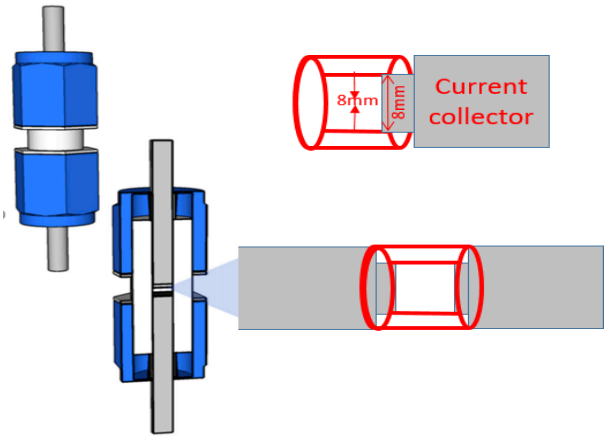

Figure S2: Schematic diagram of the Swagelok cell utilized for potentiostatic electrochemical impedance spectroscopy of bulk electrolyte solutions at open circuit voltage (25 ℃).

Table S2: Measured viscosity, reported tracer diffusivity from diaphragm cell method by Tanaka et al.1 and calculated hydrodynamic radii from Stokes-Einstein equation for several aqueous LiCl solutions at 25 ℃.

Conc. of LiCl ($mol \cdot kg^{-1}$)	Viscosity of LiCl (mPa·s)	Ion diffusion coefficient ($m^2 \cdot s^{-1}$)		Hydrodynamic radius (m)	
		Li^+	Cl^-	Li^+	Cl^-
0.1	1.042	1.02E-09	1.88E-09	2.05E-10	1.11E-10
0.5	1.110	1.01E-09	1.76E-09	1.96E-10	1.12E-10
1.03	1.199	9.31E-10	1.64E-09	1.95E-10	1.11E-10
2.1	1.394	9.14E-10	1.49E-09	1.71E-10	1.05E-10
5.6	2.032	6.15E-10	1.05E-09	1.75E-10	1.02E-10
10	4.091	4.00E-10	6.00E-10	1.33E-10	8.89E-11
13.8	8.897	2.32E-10	3.21E-10	1.06E-10	7.64E-11
18.6	18.14	1.41E-10	1.43E-10	8.53E-11	8.41E-11

Table S3: Measured viscosity, reported diffusivity from PFG-NMR by Abbas et al.[2], and calculated hydrodynamic radii from Stokes-Einstein equation for several aqueous choline fluoride solutions at 25 ℃

Conc. of ChF ($mol \cdot kg^{-1}$)	Viscosity of ChF (mPa·s)	Ion diffusion coefficient ($m^2 \cdot s^{-1}$)		Hydrodynamic radius (m)	
		Ch^+	F^-	Ch^+	F^-
1	1.328	8.80E-10	9.00E-10	1.87E-10	1.83E-10
5	2.837	4.80E-10	5.00E-10	1.60E-10	1.54E-10
10	6.174	2.50E-10	2.80E-10	1.41E-10	1.26E-10
15	8.255	8.00E-11	7.80E-11	3.30E-10	3.39E-10
20	12.05	5.00E-11	4.95E-11	3.62E-10	3.66E-10
25	17.67	2.00E-11	2.10E-11	6.17E-10	5.88E-10

Table S4: Experimental molar ionic conductivity (Λ_{EIS}) and calculated molar ionic conductivity (Λ_{NE}) for ChCl and LiTFSI

Concentration (mol·kg^{-1})	Choline chloride (mS·cm^2·mol^{-1})		LiTFSI (mS·cm^2·mol^{-1})	
	Λ_{EIS}	Λ_{NE}	Λ_{EIS}	Λ_{NE}
1	52.91	43.64	30.84	54.24
5	20.10	20.24	9.85	30.62
10	7.34	8.98	3.59	12.12
15	3.26	3.89	1.16	6.75
20	1.92	2.25	0.53	3.23

***Method S1*:** Calculation of transference number

The cation and anion transference numbers can be calculated from the ionic mobilities or diffusion coefficients of cations and anions using below the relationships.[2,3]

$$t^+ = \frac{D_+}{D_+ + D_-} = \frac{\mu_+}{\mu_+ + \mu_-}$$

$$t^- = \frac{D_-}{D_+ + D_-} = \frac{\mu_-}{\mu_+ + \mu_-}.$$

Here, D_+ and μ_+ are the diffusivity and ionic mobility of cations and D_- and μ_- are the diffusivity and ionic mobility of anions, respectively.

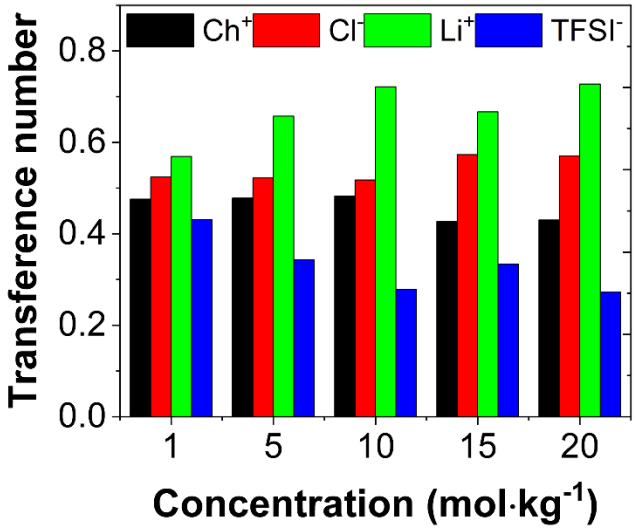

***Figure S3*:** Transference number of ions for different concentration of water-in-ChCl and water-in-LiTFSI

Method S2: Determination of the molecular volume of H_2O

Molar mass of water = 0.018 kg·mol^{-1}.

∴Number of molecules in 0.018 kg of water: $6 \cdot 10^{23}$ (Avogadro's number)

∴Mass of one molecule of water = $\frac{0.018}{6 \cdot 10^{23}}$ kg =$3 \cdot 10^{-26}$ kg

∴Volume of a water molecule = $\frac{Mass}{Density}$ = $\frac{3 \cdot 10^{-26}}{1000}$ m^3 = $3 \cdot 10^{-29}$ m^3

***Table S5*:** Hydration number of choline, chloride, lithium and TFSI ions using their effective hydrated radii (R_H) and Stokes radii (R_s).

Conc. (mol·kg^{-1})	Hydration number using effective hydrated radii R_H				Hydration number using Stokes radii R_s			
	Ch$^+$	**Cl$^-$**	**Li$^+$**	**TFSI$^-$**	**Ch$^+$**	**Cl$^-$**	**Li$^+$**	**TFSI$^-$**
1	1.27	3.83	5.94	2.35	-4.05	-4.78	0.667	1.558
5	0.76	3.58	4.12	1.62	-4.40	-4.82	0.064	0.535
10	0.28	3.41	4.45	3.13	-4.58	-4.87	0.100	2.176
15	4.99	3.29	3.92	0.41	0.06	-4.91	0.022	0.413
20	4.78	3.37	2.71	0.04	1.66	-4.89	-0.013	0.329

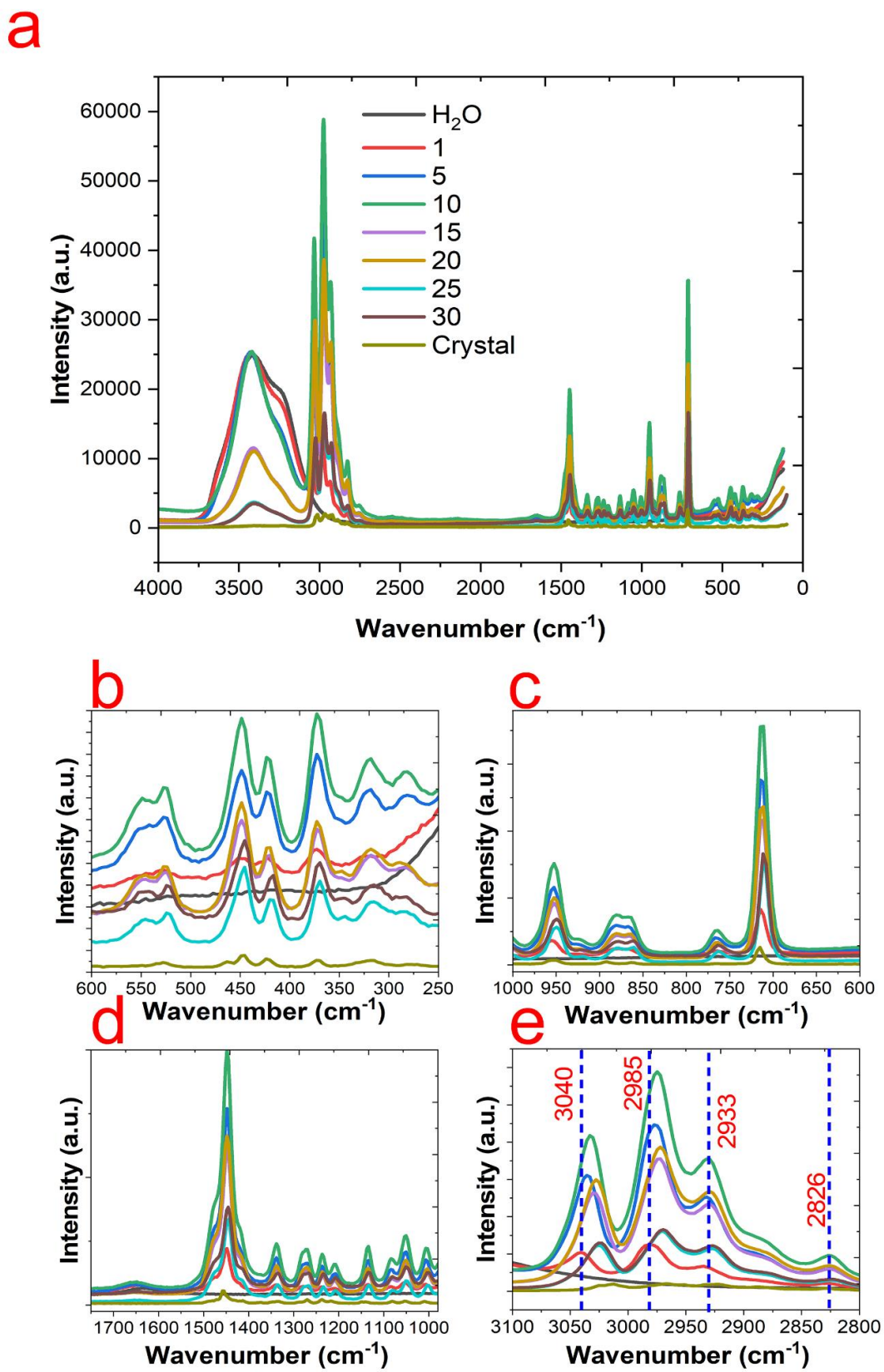

***Figure S4*:** Raman spectra of DI water, crystalline ChCl and different bulk water-in-ChCl. **a)** Full spectra over 4000-120 cm^{-1}, and enlarged solute bands over **b)** 600-250 cm^{-1}, **c)** 1000-600 cm^{-1}, **d)** 1700-980 cm^{-1}, and **e)** 3100-2800 cm^{-1}.

***Table S6*:** Assignment of the Raman bands measured from the bulk water-in-ChCl solutions over 4000-120 cm^{-1}.

Band positions (cm^{-1})	**Assignment**	**Literatures**
3420	asymmetric stretching vibration for pure water	[5]
3220	symmetric stretching vibration for pure water	
3228	weak band in the crystal ChCl, can be assigned to the O-H stretching vibration of Ch^+	
3000	C-H asymmetric stretching vibration of methyl and methylene groups	
3019	CH_3 symmetric stretching, CH_2 symmetric stretching	[6]
2917 2961	CH_2O, C–H symmetric stretching	
2811	CHO, CH stretching	
1443	CH_2 scissoring, CH_2 out of plane bending	
1450	C-H scissor rocking of methyl and methylene groups	[5]
1335	CH_2 out of plane bending	[6]
1272	CH_2 out of plane bending, COH scissoring	
1134	CH_2 out of plane bending vibration	
1049	C–C stretching	
1002	CN symmetric stretching	
951	two asymmetric stretching vibrations of C–N bonds	
877	symmetric stretching vibration of C–N bonds	
764	CH_2 in-plane rocking vibration	
711	assigned to total symmetric stretching vibration of the four C–N bonds	
720, 870	symmetric stretching vibration for C-N in crystal ChCl	[5]
705, 865	C-N vibration in aqueous ChCl solutions	
734	C-N vibration	
453	-CH- bending vibration	[6]

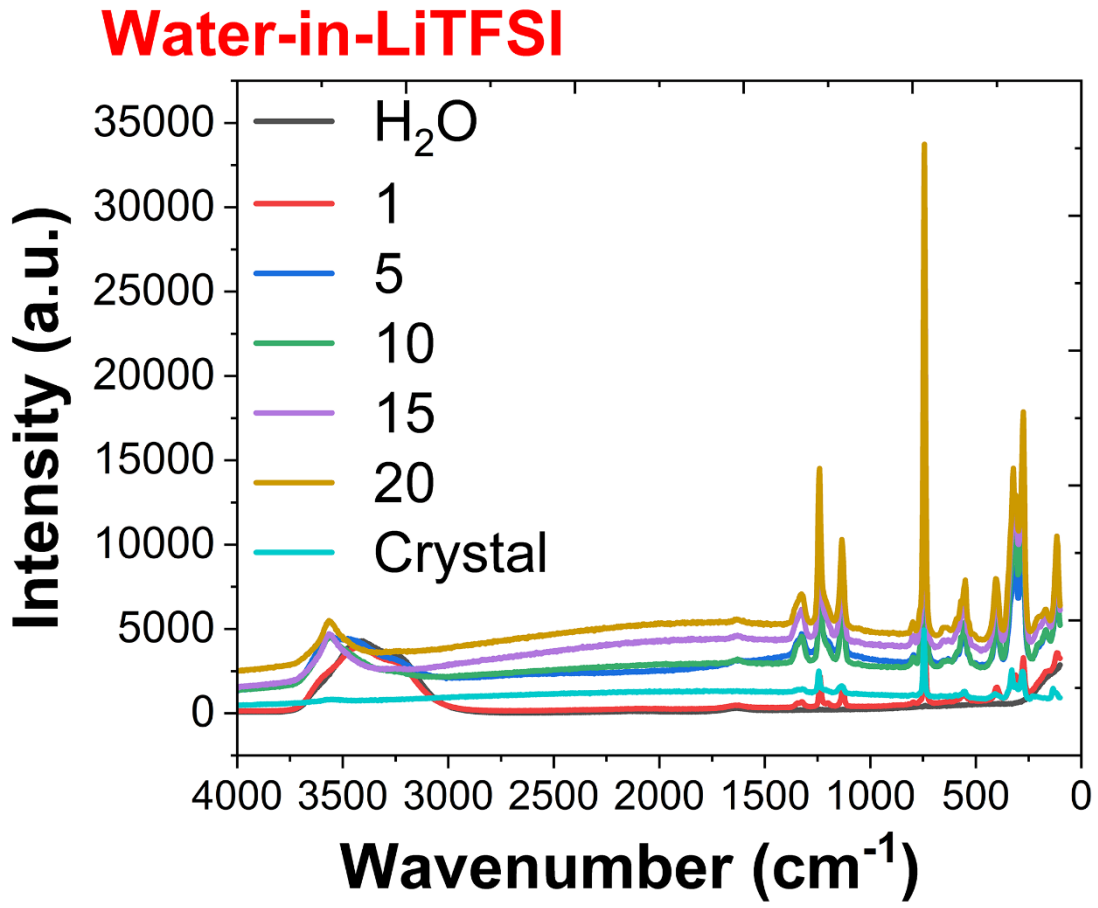

Figure S5: Raman spectra of DI water, crystalline LiTFSI and different bulk water-in-LiTFSI over 4000 to 120 cm^{-1}

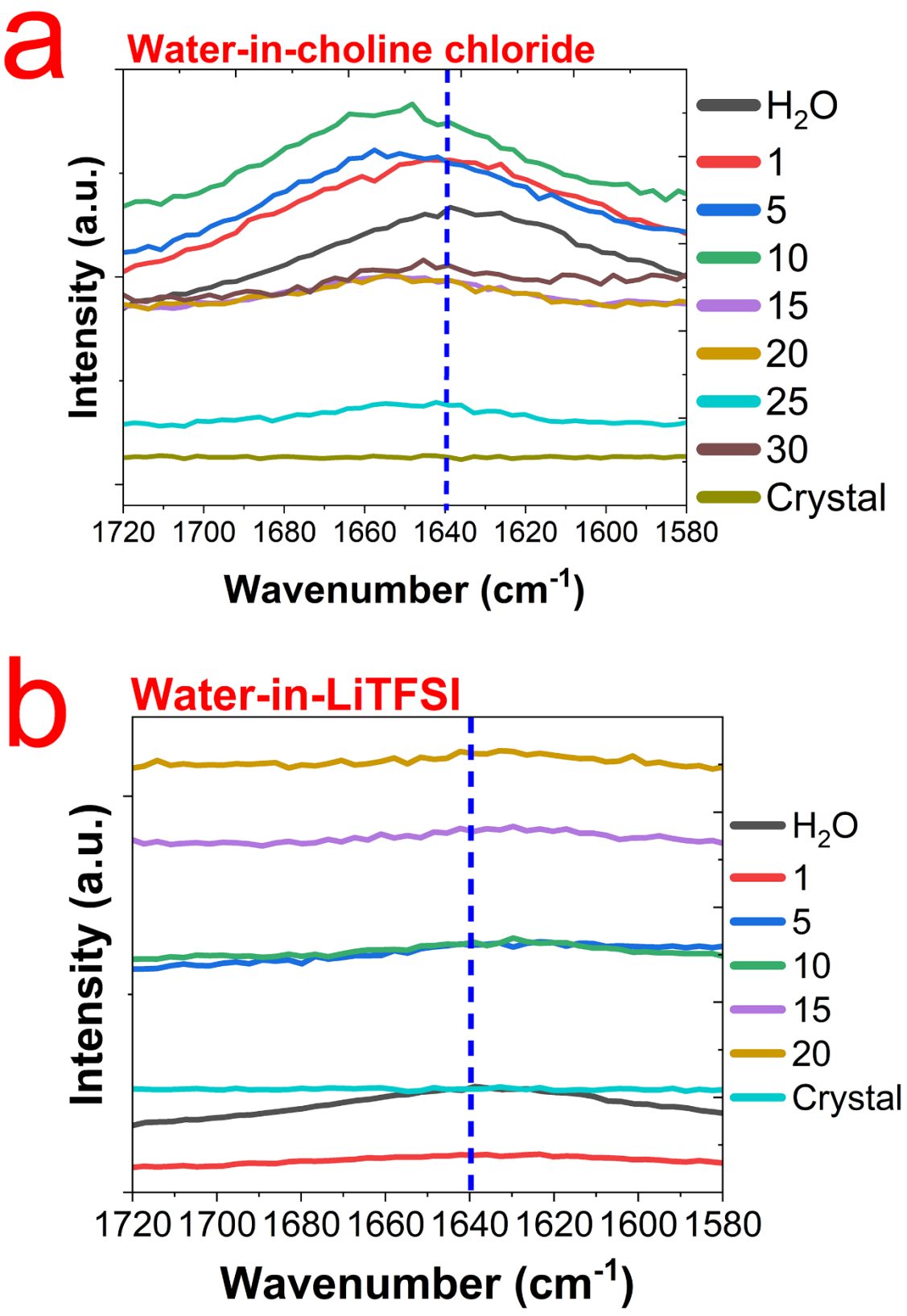

***Figure S6*:** Changes in water band at 1640 cm^{-1} for different concentrations of **a)** ChCl and **b)** LiTFSI.

Table S7: Changes of peak intensity, position and width in water band at 1640 cm^{-1} for different concentrations of ChCl.

ChCl (mol·kg^{-1})	**1640-band**		
	Intensity /a.u.	Position /cm^{-1}	Width /cm^{-1}
H_2O	94.60	1637.33	83.63
1	97.37	1643.68	90.02
5	95.32	1651.82	72.03
10	94.90	1653.04	61.96
15	96.06	1651.65	53.59
20	97.41	1651.58	51.44
25	No bands due to absence of partially H-bonded water		
30			

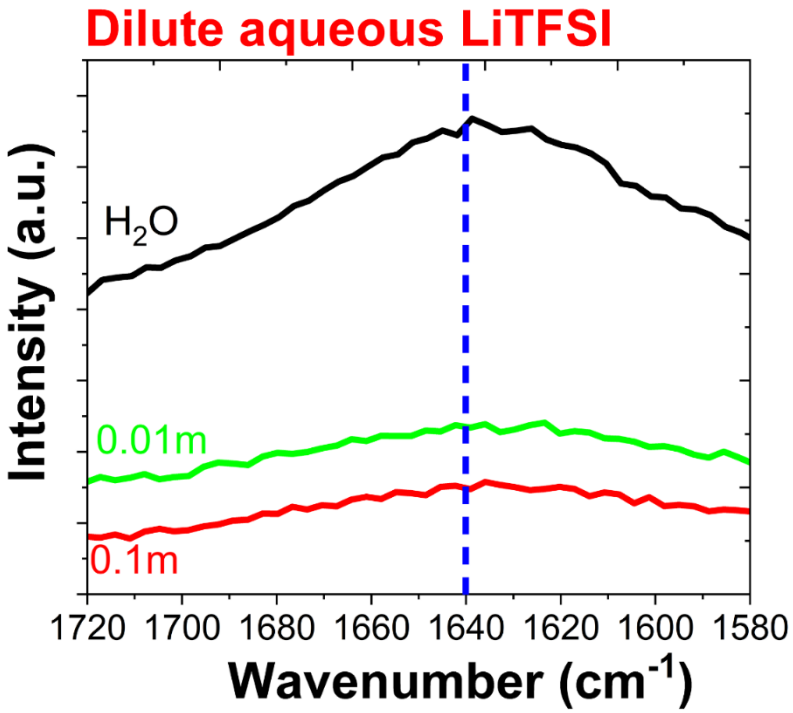

Figure S7: Evolution of water band at 1640 cm^{-1} for different diluted aqueous LiTFSI solutions.

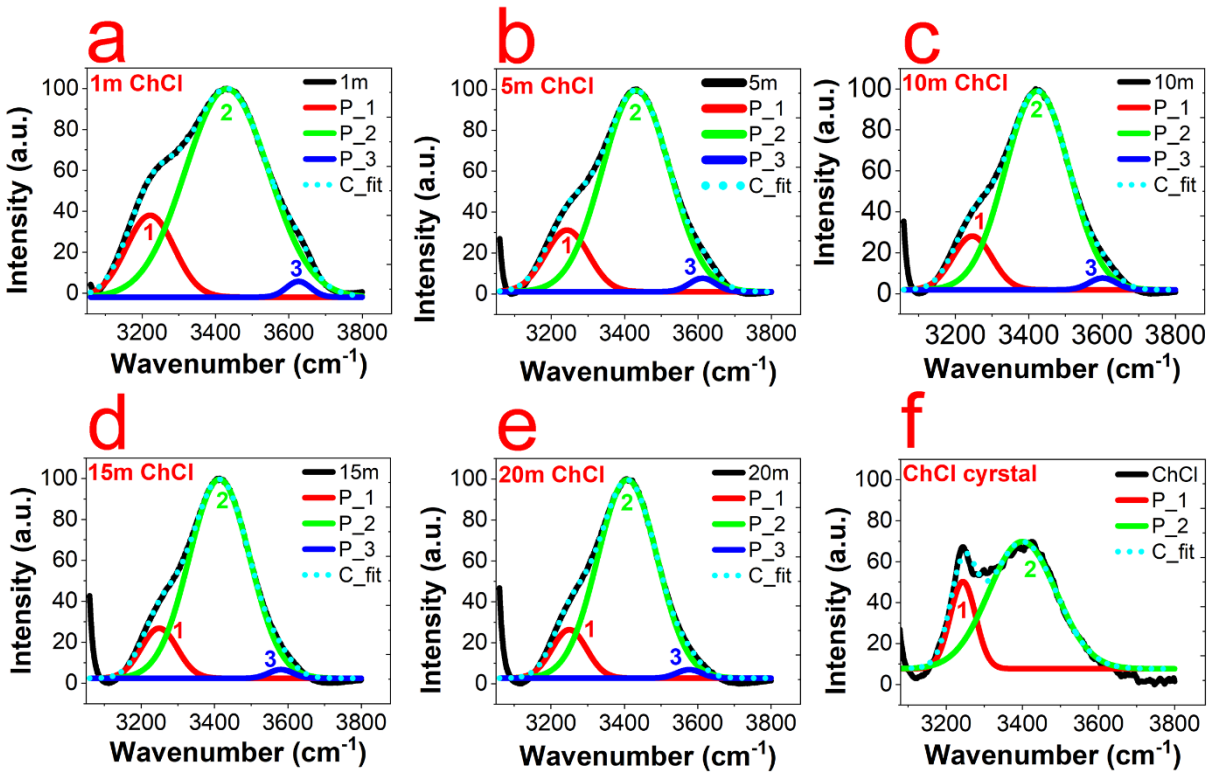

***Figure S8*:** Gaussian deconvolution of several water bands at 3220 cm^{-1}(P1-FHW), 3430 cm^{-1}(P2-PHW1), and 3610 cm^{-1} (P3-PHW2) for **a)** 1 mol·kg^{-1} ChCl, **b)** 5 mol·kg^{-1} ChCl, **c)** 10 mol·kg^{-1} ChCl, **d)** 15 mol·kg^{-1} ChCl, **e)** 20 mol·kg^{-1} ChCl, **f)** crystalline ChCl salt. Cyan dotted curve in each figure is indicating the cumulative fitting (Before deconvolution, baseline was corrected and then normalized).

Table S8: Intensity, position and width of water bands at 3220 cm^{-1}(P1), 3430 cm^{-1}(P2), and 3610 cm^{-1} (P3) for different concentrations of ChCl.

ChCl (mol·kg^{-1})	3220-band (C1)			3430-band (C2)			3610-band (C3)			Chi-square	R-square
	Intensity /a.u.	Position /cm^{-1}	Width /cm^{-1}	Intensity /a.u.	Position /cm^{-1}	Width /cm^{-1}	Intensity /a.u.	Position /cm^{-1}	Width /cm^{-1}		
H_2O	42.58 ± 0.62	3210.88 ± 0.62	166.86 ± 1.03	98.84 ± 0.49	3423.54 ± 0.49	289.16 ± 1.90	6.44 ± 0.59	3623.81 ± 0.76	82.42 ± 2.73	0.3874	0.99968
1	38.35± 0.79	3221.89 ± 0.63	154.29 ± 1.11	99.91± 0.42	3431.09 ± 0.39	267.71 ± 1.54	5.89± 0.42	3626.37 ± 0.97	77.69 ± 3.21	0.47152	0.9996
5	31.93± 0.47	3242.78 ± 2.81	139.23 ± 4.98	99.57± 0.47	3430.99 ± 1.09	217.27 ± 4.27	7.82± 0.79	3612.12 ± 4.69	84.19 ± 13.26	5.46562	0.99515
10	28.51± 0.52	3246.18 ± 3.58	125.53 ± 6.79	98.91± 0.72	3423.30 ± 1.29	206.11 ± 5.22	8.03± 0.64	3601.76 ± 7.51	86.09 ± 19.89	9.48404	0.99143
15	26.97± 0.79	3249.03 ± 4.35	114.93 ± 8.41	99.06± 0.82	3413.44± 1.55	194.84 ± 6.13	6.97± 0.52	3581.01 ± 11.47	77.56 ± 30.82	14.6620	0.98734
20	26.57± 0.62	3249.85 ± 4.88	111.04 ± 9.59	99.61± 0.48	3408.22 ± 1.79	191.70 ± 6.93	7.04± 0.82	3576.9 ± 13.731	79.82 ± 35.63	17.9695	0.98398
ChCl crystalline	50.28± 0.42	3243.57 ± 2.75	78.93 ± 7.31	69.9± 0.92	3400.01 ± 4.26	208.07 ± 11.45	No bands			97.1344	0.85089

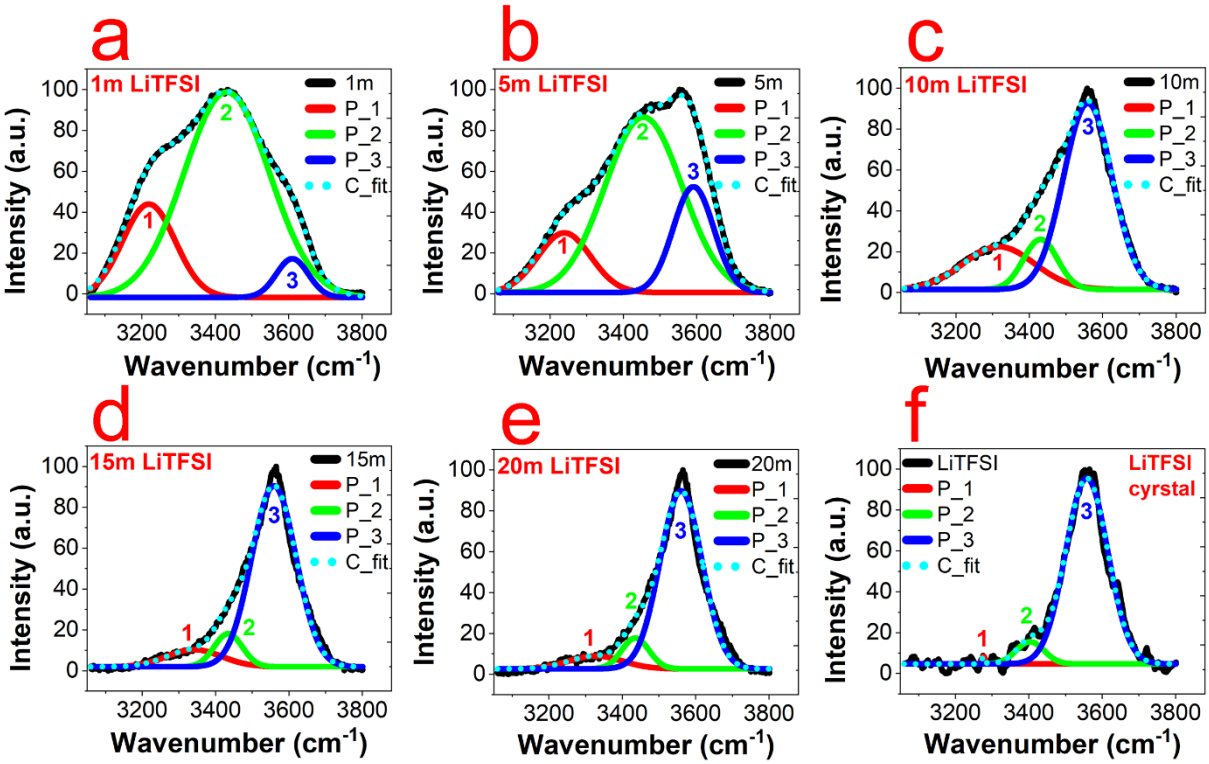

***Figure S9*:** Gaussian deconvolution of several water bands at 3220 cm^{-1}(P1), 3430 cm^{-1}(P2), and 3610 cm^{-1} (P3) for **a)** 1 mol·kg^{-1} LiTFSI, **b)** 5 mol·kg^{-1} LiTFSI, **c).** 10 mol·kg^{-1} LiTFSI, **d)** 15 mol·kg^{-1} LiTFSI, **e)** 20 mol·kg^{-1} LiTFSI, **f)** Crystalline LiTFSI salt. Cyan dotted curve in each figure indicates the cumulative fitting. Before deconvolution, baseline was corrected and then normalized.

***Table S9**:* Intensity, position and width of water bands at 3220 cm^{-1}(P1), 3430 cm^{-1}(P2), and 3610 cm^{-1} (P3) for different concentrations of LiTFSI.

LiTFSI (mol·kg^{-1})	3220-band			3430-band			3610-band			Chi-square	R-square
	Intensity /a.u.	Position /cm^{-1}	Width /cm^{-1}	Intensity /a.u.	Position /cm^{-1}	Width /cm^{-1}	Intensity /a.u.	Position /cm^{-1}	Width /cm^{-1}		
H_2O	42.58 ± 0.62	3210.88 ± 0.62	166.86 ± 1.03	98.84 ± 0.49	3423.54 ± 0.49	289.16 ± 1.90	6.44 ± 0.59	3623.81 ± 0.76	82.42 ± 2.73	0.3874	0.99968
1	43.71 ± 0.79	3218.96 ± 0.89	169.22 ± 1.23	97.84 ± 0.41	3431.36 ± 0.52	274.43 ±3.02	17.50 ± 0.79	3609.95 ± 0.56	102.64 ± 2.42	0.5135	0.99955
5	29.79 ± 0.42	3239.17 ± 1.81	169.19 ± 2.28	89.67 ± 0.78	3454.98 ± 2.34	247.91 ± 6.07	52.24 ± 0.91	3591.14 ± 0.54	130.49± 2.52	0.8173	0.99928
10	22.23± 0.91	3317.05 ± 11.02	228.35 ± 16.65	26.13± 0.65	3430.40 ± 2.23	109.02 ± 7.21	92.78± 0.69	3559.42 ± 0.94	155.61 ± 1.89	2.6747	0.99687
15	10.71± 0.62	3341.71 ± 36.1	176.27 ± 51.89	19.43± 0.79	3434.48 ± 3.85	90.17 ±13.52	91.32± 0.73	3558.94 ± 0.95	142.29 ± 2.08	6.48394	0.99179
20	8.91± 0.52	3327.19 ± 32.22	172.05± 57.39	17.89± 0.42	3435.62 ± 4.40	87.38 ±13.58	87.96± 0.42	3560.19 ± 0.97	135.05 ± 2.29	9.04132	0.98774
LiTFSI crystalline	8.37± 0.41	3276.85 ± 3.03	9.97 ± 7.19	15.63± 0.62	3403.35± 4.05	89.56± 9.44	95.26± 0.49	3557.95 ± 0.58	135.29 ± 1.55	10.73464	0.98685

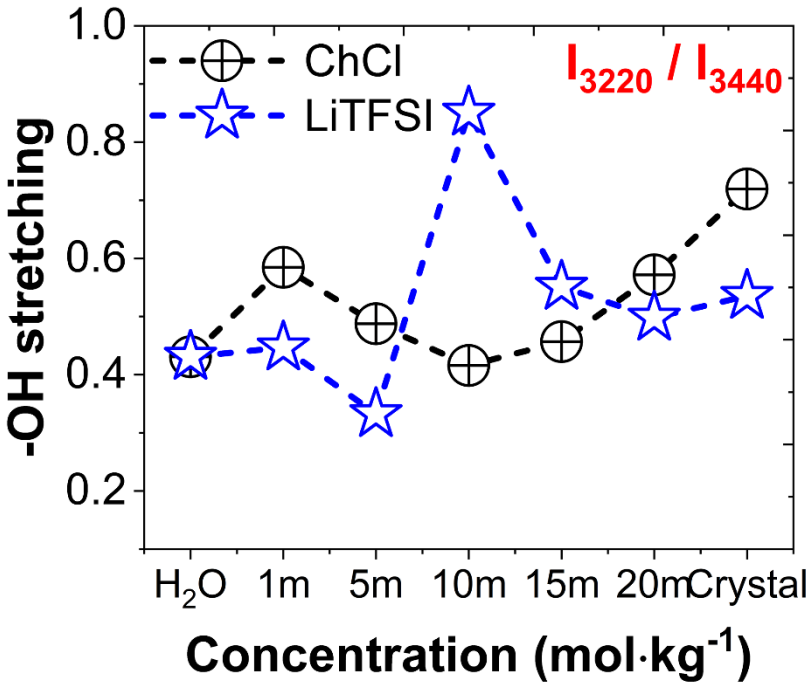

***Figure S10*:** Intensity ratio of the -OH stretching bands at 3200 cm^{-1} (I_{3220}) and 3440 cm^{-1} (I_{3440}) for ChCl and LiTFSI. Connecting dotted lines are guide to the eye.

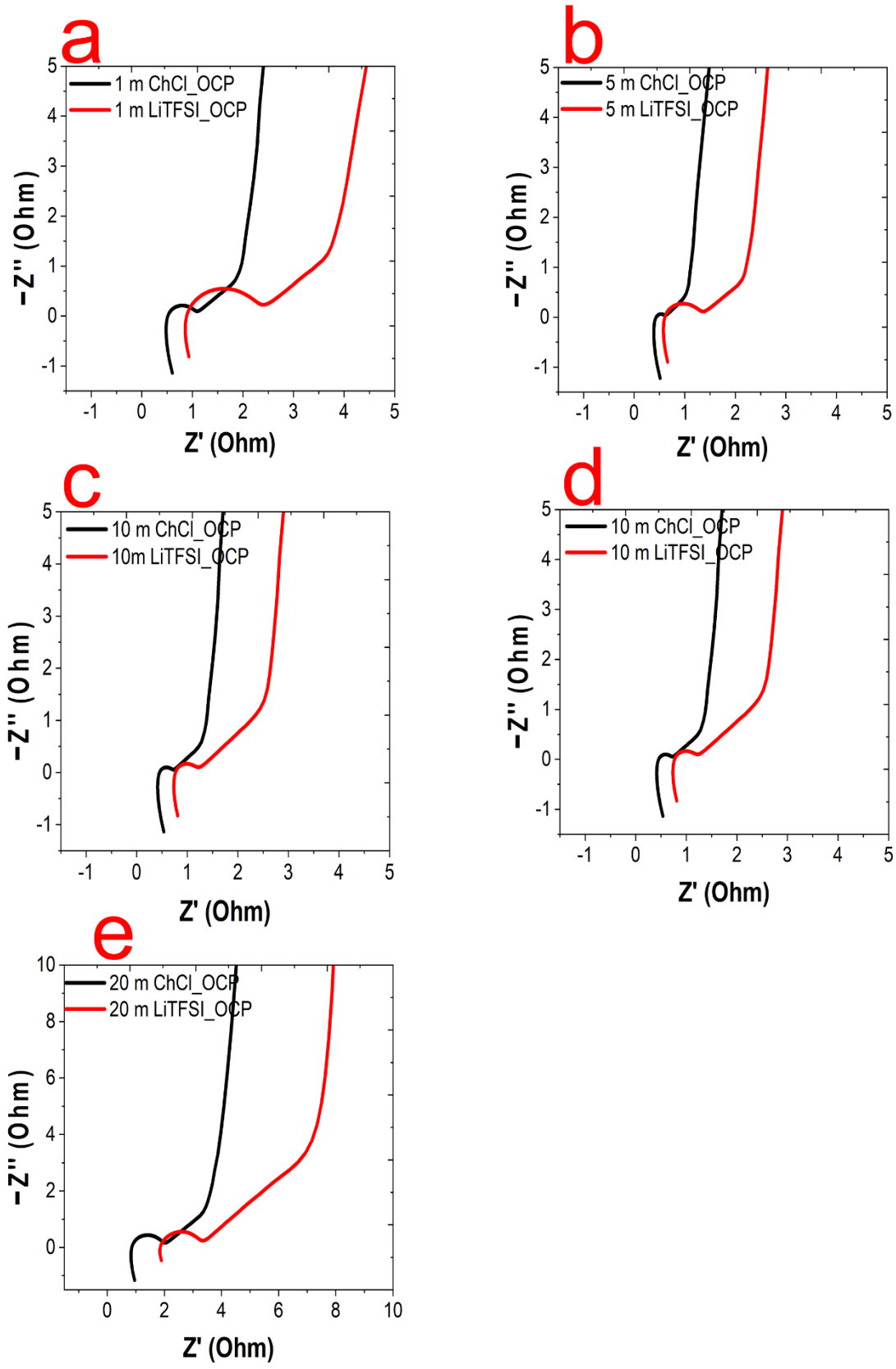

***Figure S11*:** Nyquist plots of the electrochemical impedance spectra of capacitor cells operating under open circuit potential (≈30 mV) for different concentrations of ChCl and LiTFSI **a)** 1, **b)** 5, **c)** 10, **d)** 15, and **e)** 20 mol·kg^{-1}.

***Table 10*:** Equivalent series resistance (ESR), charge transfer resistance (CTR), equivalent distribution resistance (EDR), and ion diffusion resistance (IDR) of the capacitor cells operated at open circuit potential (≈30 mV) for different concentrations of ChCl and LiTFSI.

Conc. (mol·kg^{-1})	Voltage (V)	ESR (Ohm)		CTR (Ohm)		EDR (Ohm)		IDR (Ohm)	
		ChCl	LiTFSI	ChCl	LiTFSI	ChCl	LiTFSI	ChCl	LiTFSI
1	OCP	0.60	0.93	0.49	1.47	1.64	3.50	0.89	1.53
5		0.51	0.66	0.12	0.69	0.84	1.89	0.43	0.86
10		0.53	0.81	0.20	0.43	1.18	2.20	0.65	1.46
15		0.64	1.35	0.60	1.19	1.91	4.80	0.99	2.70
20		0.96	1.90	1.07	2.47	3.20	7.96	1.67	4.18

Method S3: Analysis of capacitance from EIS

Angular frequency: $\omega = 2\pi \cdot F$ ***(S1)***

Real part of the permittivity: $\in' = \frac{t}{A \cdot \omega \cdot \epsilon_0} \cdot \frac{Z''}{Z'^2 + Z''^2}$ ***(S2)***

Imaginary part of the permittivity: $\in'' = \frac{t}{A \cdot \omega \cdot \epsilon_0} \cdot \frac{Z'}{Z'^2 + Z''^2}$ ***(S3)***

Capacitance of ideal capacitor in vacuum: $C_0 = \frac{A \cdot \in_0}{t}$ ***(S4)***

Real capacitance: $C' = \in' \cdot C_0$ ***(S5)***

Imaginary capacitance: $C'' = \in'' \cdot C_0$ ***(S6)***

Here, F is the characteristic frequency, A is the geometric area of the carbon electrode; t is the thickness of the carbon electrode; Z' is the real component of the impedance; Z'' is the imaginary component of the impedance, and $\in_0$ is the vacuum permittivity.

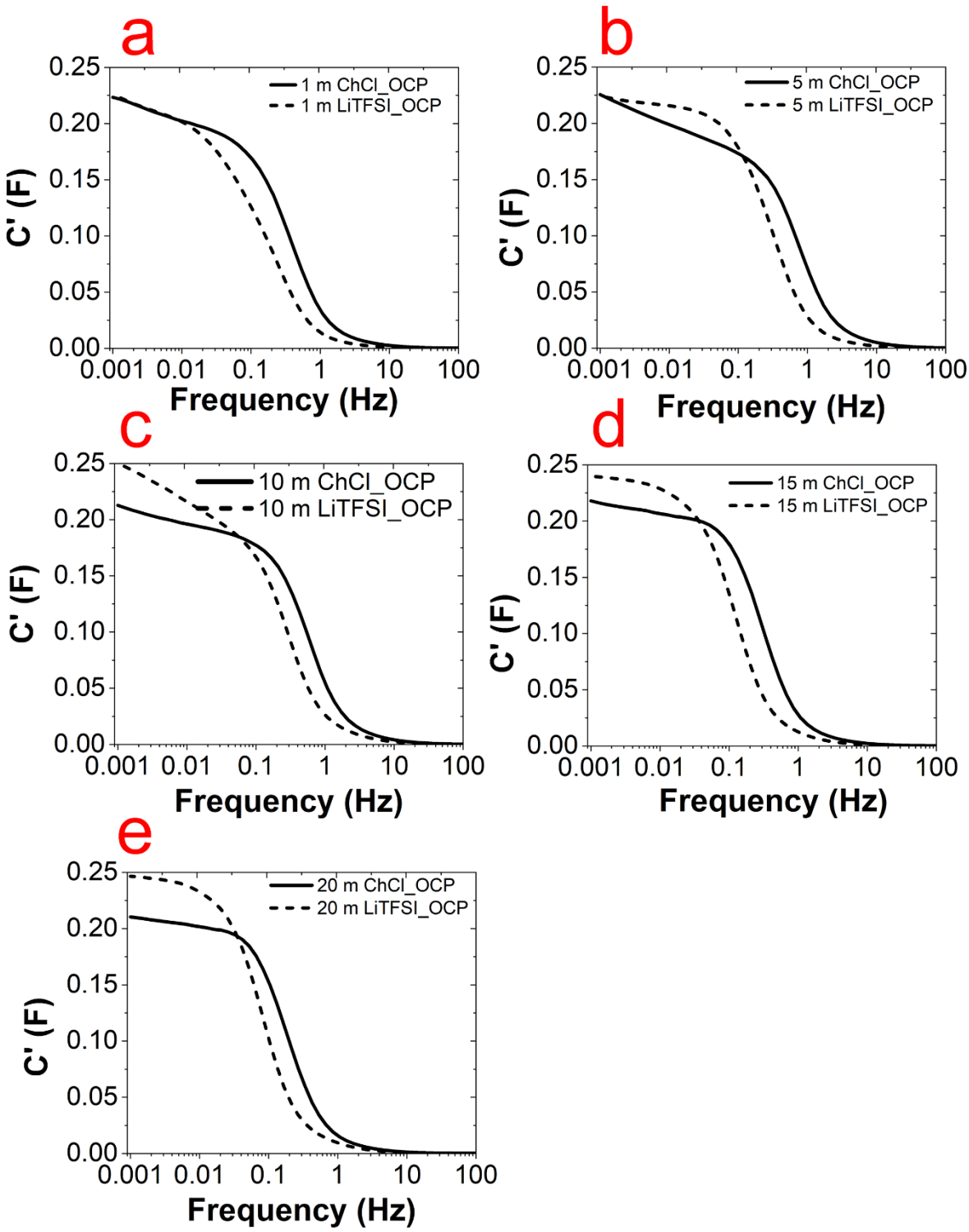

Figure S12: Real capacitance (C') from EIS of capacitor cells operating under open circuit potential for different concentrations of ChCl and LiTFSI a) 1 m, b) 5 m, c) 10 m, d) 15 m, and e) 20 mol·kg^{-1}.

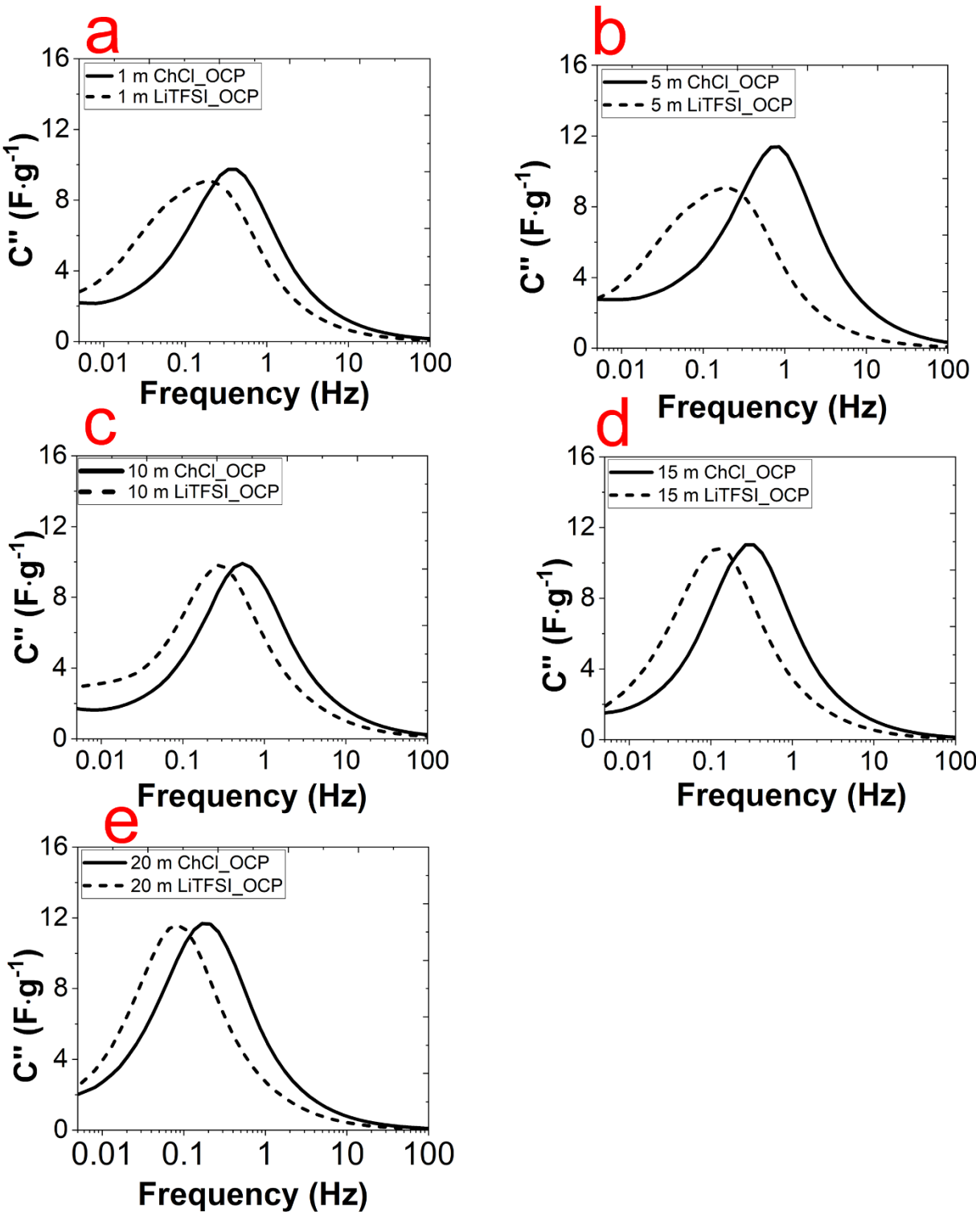

Figure S13: Imaginary capacitance (C'') from EIS of capacitor cells operating open circuit potential for different concentrations of ChCl and LiTFSI a) 1, b) 5, c) 10, d) 15, and e) 20 mol·kg^{-1}.

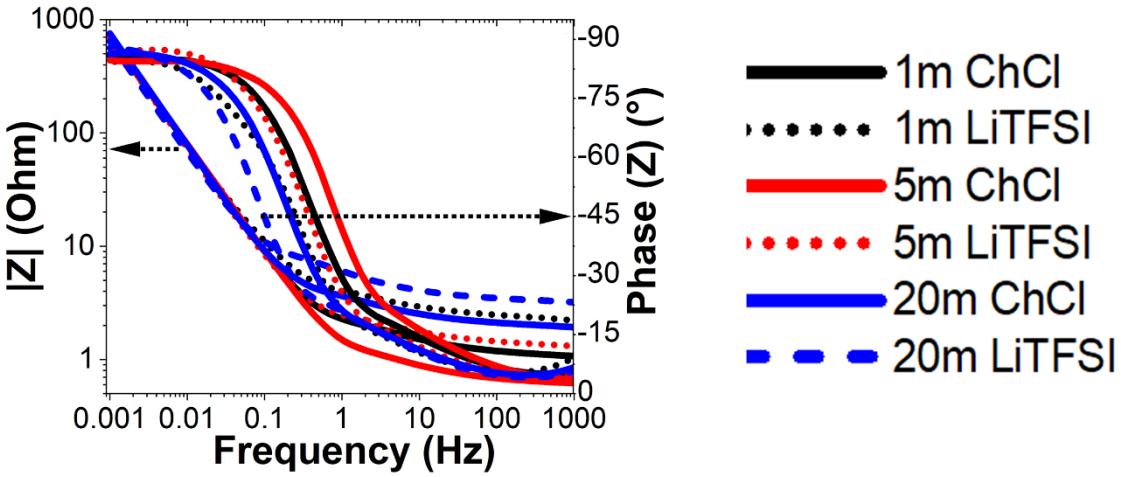

***Figure S14*:** Bode plots of electrochemical impedance spectra of capacitor cells operating under open circuit potential for different concentrations of ChCl and LiTFSI

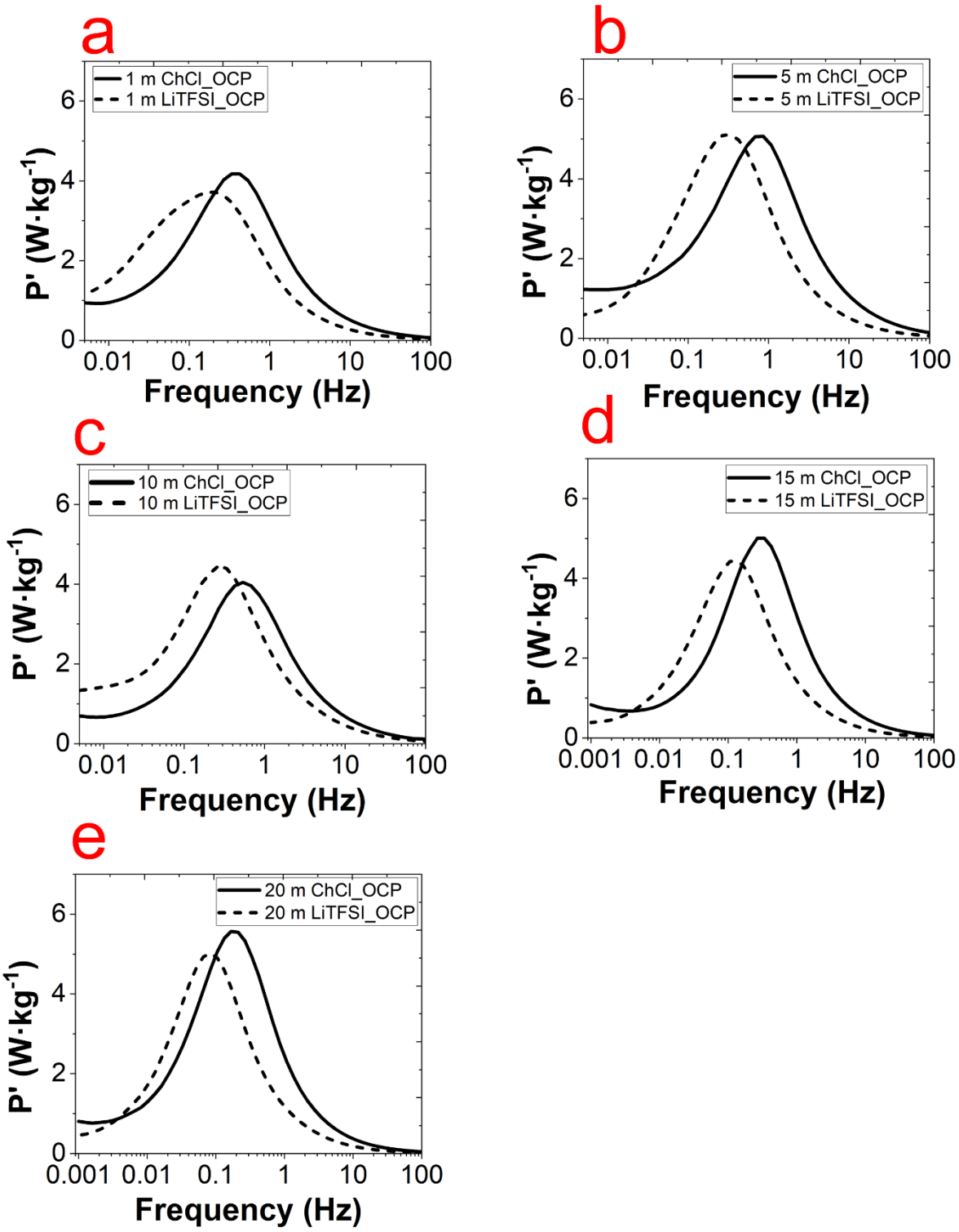

***Figure S15*:** Real power (P') from EIS of capacitor cells operating under open circuit potential for different concentrations of ChCl and LiTFSI **a)** 1, **b)** 5, **c)** 10, **d)** 15, and **e)** 20 mol·kg^{-1}.

***Table S11*:** Effect of salt concentration on the bulk electrolyte conductivity, in-pore ionic conductivity, bulk and in-pore ionic resistance, bulk to in-pore conductivity ratio, capacitance, and power density of capacitor cells under open circuit potential

Salt conc. (mol/kg)	$\sigma_{in\text{-}bulk}$ (mS/cm)	$\sigma_{in\text{-}pore}$ (mS/cm)	$R_{in\text{-}bulk}$ (Ohm·cm)	$R_{in\text{-}pore}$ (Ohm·cm)	σ_{bulk} / $\sigma_{in\text{-}pore}$ or $R_{in\text{-}pore}$ to $Ri_{in\text{-}bulk}$	D_{bulk} / $D_{in\text{-}pore}$		C''_{max} (mF)	C''_{max} (mF/cm^2)	C'_{max} (F·g^{-1})	P'_{max} (W/kg)
						Micro	Meso				
1 ChCl	56.8	2.59	17.61	386.3	21.9	29.9	3.4	83.7	106.6	9.74	4.16
1 LiTFSI	31.25	1.53	32.0	652.7	20.4	27.8	3.1	73.8	94.0	9.05	3.72
5 ChCl	100	5.32	9.93	187.8	18.9	32.5	3.6	81.3	103.5	11.37	**5.11**
5 LiTFSI	52.89	2.22	18.9	451.0	23.85	25.7	2.9	89.2	113.5	10.83	**5.08**
10 ChCl	77.1	5.25	12.97	190.3	14.7	22.9	2.6	86.5	110.2	9.91	4.04
10 LiTFSI	38.34	2.28	26.1	438.8	16.82	20.0	2.2	87.9	111.9	9.81	4.45
15 ChCl	63.1	2.29	15.85	437.0	27.6	23.8	2.7	95.5	121.6	11.03	5.02
15 LiTFSI	19.25	1.10	51.9	907.5	17.47	37.5	4.2	99.4	126.6	10.81	4.45
20 ChCl	40.8	1.50	24.49	668.8	27.3	16.6	1.9	92.9	118.3	11.68	**5.58**
20 LiTFSI	11.10	0.91	90.1	1100.2	12.22	37.2	4.2	104.4	132.9	11.60	**4.96**

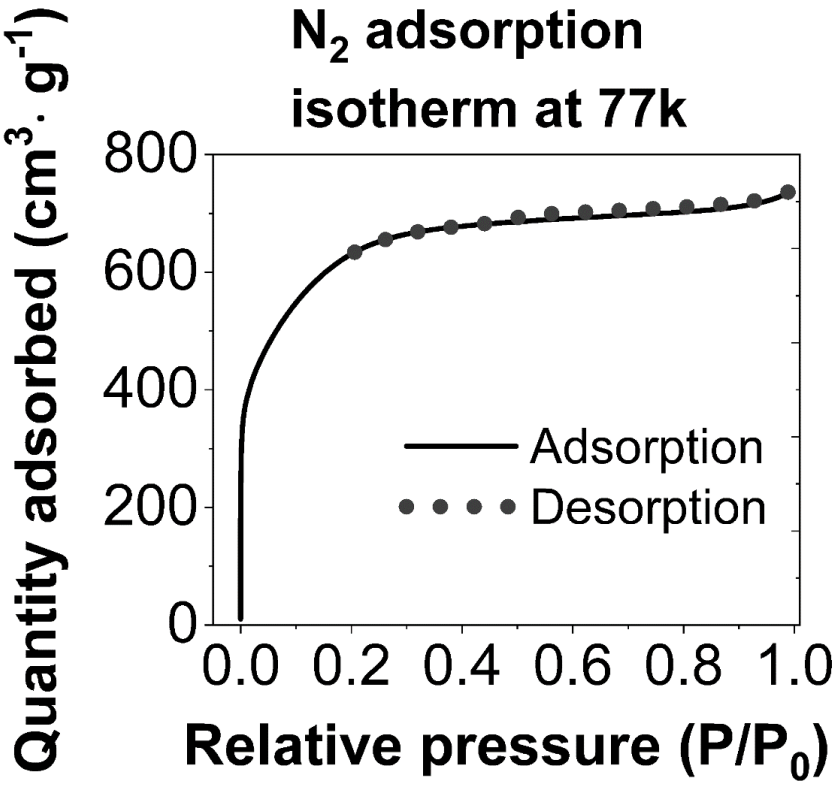

***Figure S16*: N**itrogen gas adsorption and desorption isotherm of YP80 F carbon electrode at 77 K.

Method S4: Determination of ion-pair (mutual) diffusivity from self-ion diffusivity[7]

According to the Nernst-Einstein equation, diffusivity of ion-pair D_σ using the experimental molar ionic conductivity Λ_{NE} can be derived from **equation 7**

$$D_\sigma = \frac{N_A \cdot e^2}{k_B \cdot T} \cdot \Lambda_{EIS} \qquad \textbf{S7}$$

Here, N_A is Avogadro's number (6.023×10^{23} mol^{-1}), e is the elementary charge (1.602×10^{-19} C),

In addition, effective ionic diffusivities can be calculated from the PFG-NMR based self-ion diffusivity using **equations S8** and **S9**

$$D_+^{eff} = \frac{1}{2}(D_\sigma + D_+^{NMR} - D_-^{NMR}) \qquad \textbf{S8}$$

$$D_-^{eff} = \frac{1}{2}(D_\sigma + D_-^{NMR} - D_+^{NMR}) \qquad \textbf{S9}$$

As such we not only just separated the charged species from the neutral aggregates, but also eliminated part of the ionic diffusivities associated with interaction (friction) between ions whatsoever, even in the case where they did not form a complex with each other. In this regard, D_+^{eff} and D_-^{eff} would represent binary diffusivities required for the implementation of the concentrated solution theory based on the Onsager−Stefan−Maxwell formalism with **equation S10**[7]

$$D_{+-} = \frac{1}{2}(D_+^{eff} + D_-^{eff}) \qquad \textbf{S10}$$

***Table S12*:** Diffusivity of ions and water in bulk electrolyte, effective in-pore diffusivity of ions and water, tortuosity, $R_{in\text{-}pore}$, C''_{max} within the micro and meso pores together with their cell time-constants and knee frequencies for different salt concentrations under open circuit potential.

Salt (mol·kg^{-1})	D_{bulk} (10^{-11} · m^2·s^{-1})		Effective $D_{in\text{-}pore}$ (10^{-11} · m^2·s^{-1})				Effective Tortuosity		Effective $R_{in\text{-}pore}$ (Ohm·cm^2)		C''_{max} (F·g^{-1})		Time constant (ms)	F (mHz)	C''_{max} (F·g^{-1}) from EIS	$R_{in\text{-}pore}$ (Ohm·cm^2) from EIS
	Salts	H_2O	ChCl or LiTFSI		H_2O											
			Micro	Meso	Micro	Meso	Micro	Meso	Micro	Meso	Micro	Meso				
1 m ChCl	70.56	190.1	2.36	21.02	6.36	56.63	25.48	0.50	2.10	18.75	96.55	10.84	353.9	449.7	9.74	20.86
1 m LiTFSI	41.13	101.2	1.48	13.37	3.64	32.37	23.70	0.46	3.56	31.69	89.65	10.07	527.4	301.8	9.05	35.25
5 m ChCl	26.80	144.3	1.04	9.27	5.59	49.79	21.97	0.43	1.02	9.12	112.7	12.65	167.0	952.8	11.37	10.14
5m LiTFSI	13.14	80.1	0.41	3.66	2.46	21.92	27.72	0.54	2.46	21.90	107.2	12.04	440.0	361.7	10.83	24.36
10 m ChCl	9.79	82.74	0.33	2.95	4.14	36.83	17.05	0.33	1.04	9.24	98.25	11.03	180.2	883.0	9.91	10.28
10 m LiTFSI	4.79	27.6	0.21	1.91	1.18	10.49	19.54	0.38	2.39	21.30	97.17	10.92	421.9	377.2	9.81	23.69
15 m ChCl	4.35	50.5	0.12	1.03	1.35	11.97	32.03	0.63	2.38	21.21	109.3	12.27	456.7	348.5	11.03	23.60
15 m LiTFSI	1.55	12.5	0.07	0.59	0.50	4.49	20.30	0.39	4.95	44.06	107.0	12.02	987.3	161.2	10.81	49.01
20 m ChCl	2.56	35.1	0.07	0.61	0.94	8.40	31.73	0.62	3.64	32.47	115.8	13.00	679.9	234.1	11.68	36.12
20 m LiTFS	0.71	10.1	0.04	0.33	0.61	5.40	14.20	0.27	6.00	53.42	114.8	12.90	1256.7	126.6	11.60	59.41

***Table S13*:** In-pore diffusivity of the organic electrolytes PET_4BF_4 and $TEABF_4$ determined by in-situ NMR and electrochemical techniques. Borchardt et al. followed three methods[8-10] based on EIS to compare their in-situ NMR diffusivity values within micro, meso, and hierarchical pores.[11]

Parameters	**Forse *et al.* (10^{-11}·m^2·s^{-1})**[12]		**Borchardt *et al.* (10^{-11}·m^2·s^{-1})**[11]					
Methods	In-situ NMR		In-situ NMR			EIS (following Armstrong et al.)[10]	EIS (following van Aken *et al.)*[9]	EIS (following Ahuja model)[8]
Carbon types	YP50F and YP80F		Including YP50F and YP80F					
Electrolytes	1.5 M PET_4BF_4		1 M $TEABF_4$ in ACN			1 M $TEABF_4$		
	PET_4^+	BF_4^-	TEA^+	BF_4^-	ACN			
D_{bulk}	-	-	117	142	439	TEA^+ + BF_4^- + acetonitrile ≈698		
$C_{micro\ (YP80F)}$	-	0.7-1.0	0.17	0.20	13	0.12	2400	0.12
$C_{hierarch}$	-	-	0.087	0.27	40	16	11000	0.15
$C_{meso\ (YP50F)}$	0.12 to 0.32	0.30-0.55	9	12	60	5.2	4600	0.39

***Table S14*:** Ion-pair size (nm) in ChCl and LiTFSI with corresponding cumulative surface area (CSA) at pore width similar to ion pair size and cumulative surface area (CSA%) for different salt concentrations.

Ion pair type	Salt conc. (mol/kg)	Size of ion pair (nm)	Total CSA (m^2/g)	CSA at the pore width similar to ion pair size (m^2/g)	CSA%
Cation-cation in ChCl	**1**	0.723	1735.5	479.02	27.60
	5	0.688		415.44	23.94
	10	0.671		384.52	22.16
	15	0.846		700.31	40.35
	20	0.945		850.61	49.01
Anion-anion in ChCl	**1**	0.644	1735.5	340.77	19.64
	5	0.632		316.07	18.21
	10	0.624		304.07	17.52
	15	0.618		290.06	16.71
	20	0.622		298.09	17.18
Cation-anion in ChCl	**1**	0.682	1735.5	410.44	23.65
	5	0.656		364.28	20.99
	10	0.647		340.77	19.64
	15	0.729		490.54	28.27
	20	0.781		597.56	34.43
Cation-cation in LiTFSI	**1**	0.701	1735.5	449.97	25.93
	5	0.623		298.086	17.18
	10	0.636		329.97	19.01
	15	0.612		278.24	16.03
	20	0.543		160.12	9.23
Anion-anion in LiTFSI	**1**	0.744	1735.5	531.54	30.63
	5	0.718		479.03	27.60
	10	0.772		573.56	33.05
	15	0.671		390.54	22.50
	20	0.654		361.28	20.82
Cation-anion in LiTFSI	**1**	0.722	1735.5	489.02	28.18
	5	0.669		389.52	22.45
	10	0.703		449.97	25.93
	15	0.641		334.77	19.29
	20	0.597		261.23	15.05

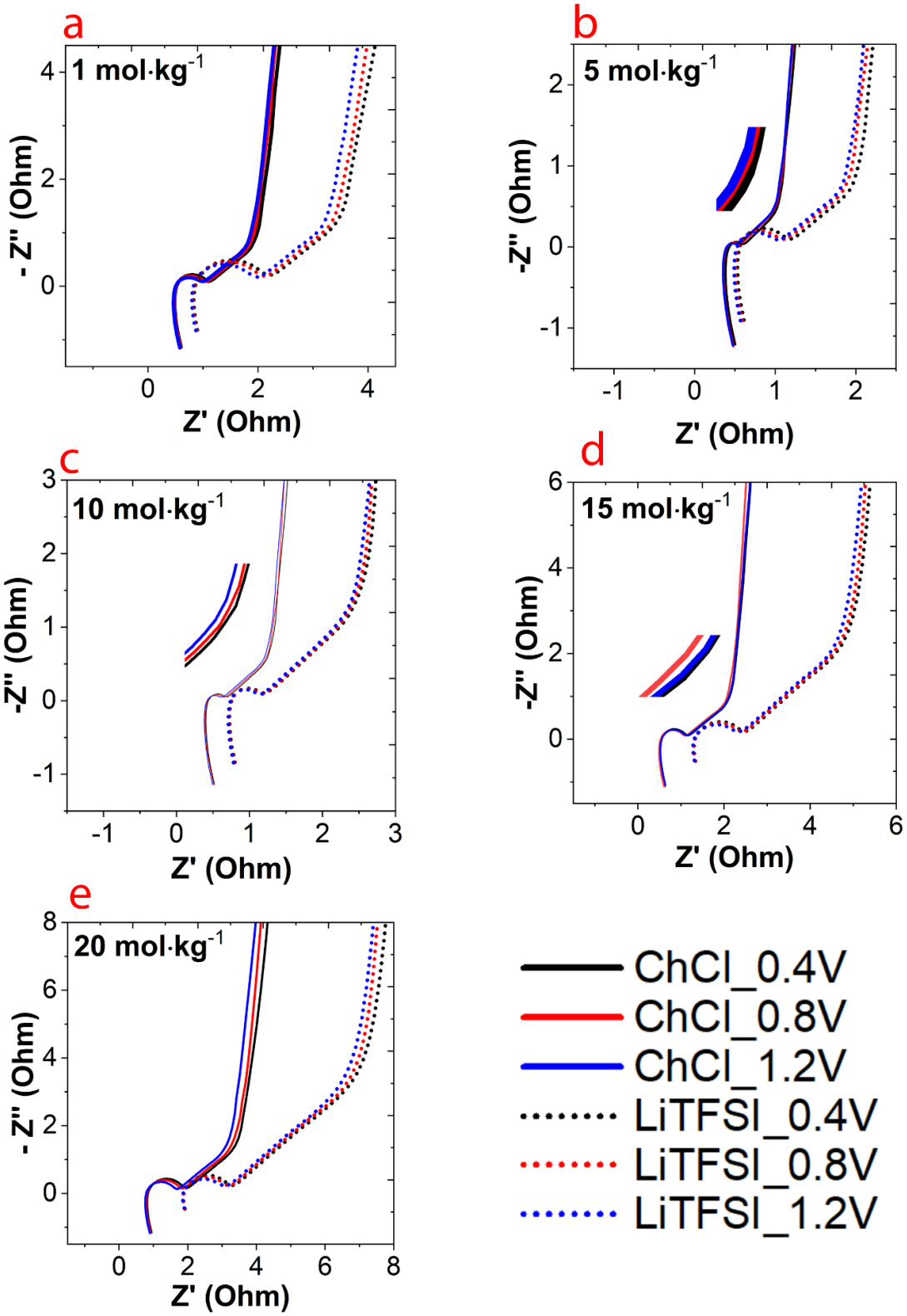

***Figure S17*:** Nyquist plots of the electrochemical impedance spectra of the capacitor cells operating under different bias voltage for different concentrations of ChCl and LiTFSI **a)** 1, **b)** 5, **c)** 10, **d)** 15, and **e)** 20 mol·kg^{-1}.

***Table S15*:** Equivalent series resistance (ESR), charge transfer resistance (CTR), equivalent distribution resistance (EDR), and ion diffusion resistance (IDR) from the capacitor cells operating under different bias voltage for different concentrations choline chloride and LiTFSI

Salt conc. ($mol \cdot kg^{-1}$)	Applied potential (V)	ESR (Ohm)		CTR (Ohm)		EDR (Ohm)		IDR (Ohm)	
		ChCl	LiTFSI	ChCl	LiTFSI	ChCl	LiTFSI	ChCl	LiTFSI
1	0.4	0.60	0.90	0.51	1.30	1.68	3.23	0.91	1.43
	0.8	0.59	0.88	0.44	1.21	1.61	3.14	0.90	1.38
	1.2	0.58	0.87	0.39	1.10	1.58	2.98	1.00	1.33
5	0.4	0.50	0.61	0.10	0.56	0.81	1.70	0.44	0.84
	0.8	0.48	0.59	0.07	0.49	0.78	1.64	0.47	0.83
	1.2	0.47	0.57	0.04	0.46	0.76	1.56	0.49	0.79
10	0.4	0.52	0.80	0.17	0.41	1.13	2.12	0.65	1.44
	0.8	0.51	0.79	0.13	0.40	1.03	2.08	0.66	1.36
	1.2	0.50	0.78	0.10	0.36	1.00	2.00	0.67	1.29
15	0.4	0.63	1.33	0.53	1.15	1.87	4.57	1.05	2.65
	0.8	0.61	1.33	0.47	1.04	1.80	4.52	1.07	2.63
	1.2	0.64	1.31	0.46	1.00	1.84	4.33	1.06	2.54
20	0.4	0.94	1.92	0.98	2.34	3.15	7.66	1.63	4.08
	0.8	0.92	1.91	0.90	2.23	3.02	7.48	1.65	4.01
	1.2	0.90	1.90	0.77	2.16	2.87	7.19	1.63	3.84

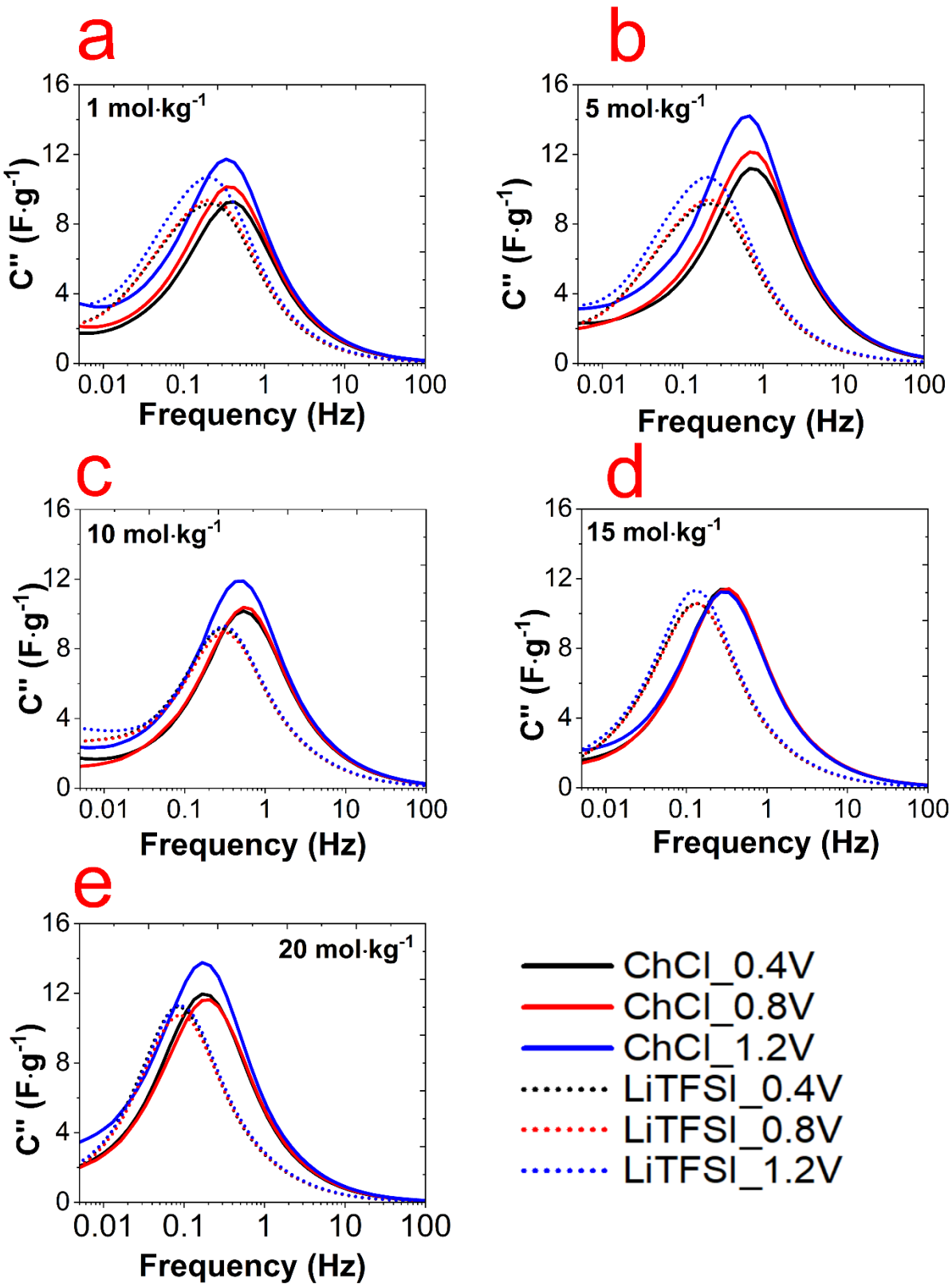

Figure S18: Imaginary capacitance (C'') from EIS of capacitor cells operating under different bias voltages for different concentrations of ChCl and LiTFSI a) 1, b) 5, c) 10, d) 15, and e) 20 mol·kg-^{1}

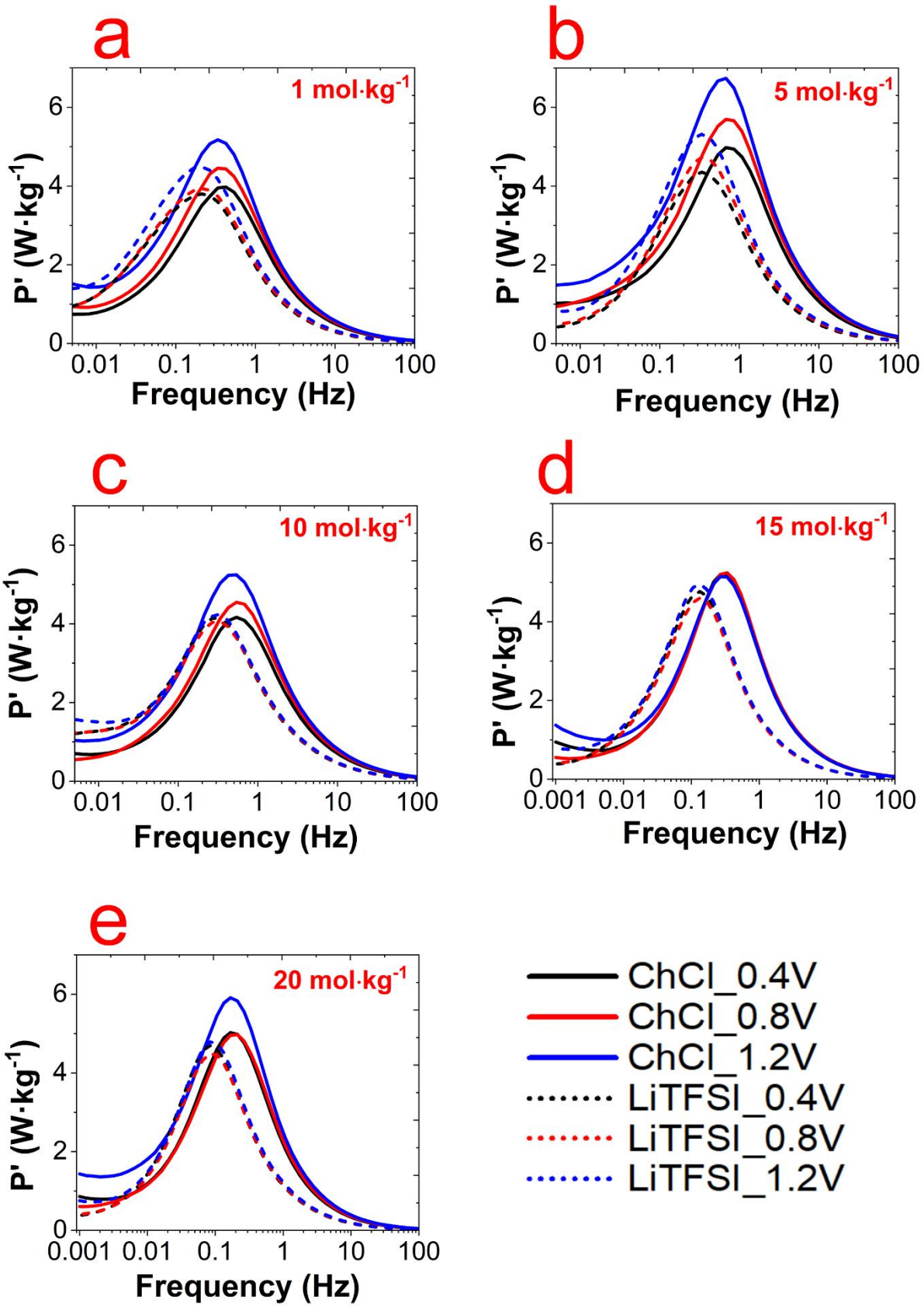

Figure S19: Real power (P') from EIS of capacitor cells operating under different bias voltages for different concentrations of ChCl and LiTFSI a) 1, b) 5, c) 10, d) 15, and e) 20 mol·kg^{-1}.

Table S16: Effect of salt concentration and applied voltage on the effective in-pore ion diffusivity, tortuosity, Rin-pore, C′′max in the micro and meso pores together with their cell time-constant values and knee frequencies

Salt (mol·kg^{-1})	Applied potential (V)	D_{bulk} (10^{-11} · m^2·s^{-1})	Effective $D_{in\text{-}pore}$ (10^{-11} · m^2·s^{-1})		Effective Tortuosity		$R_{in\text{-}pore}$ (Ohm·cm^2)			C''_{max} (F·g^{-1})			Time constant (ms)	F (mHz)	P'_{max} (W·kg^{-1})
			Micro	Meso	Micro	Meso	Micro	Meso	Total from EIS	Micro	Meso	Total from EIS			
1 m ChCl	0.4	70.56	2.407	21.425	25.52	0.50	2.22	19.75	21.97	91.91	10.32	9.27	354.9	448.5	3.98
	0.8		2.738	24.374	22.44	0.44	1.95	17.34	19.29	100.3	11.27	10.13	340.2	467.8	4.47
	1.2		3.251	28.941	18.90	0.37	1.65	14.74	16.40	116.2	13.04	11.72	334.9	475.2	5.19
1 m LiTFSI	0.4	41.13	1.630	14.724	21.53	0.42	3.39	30.19	33.58	90.94	10.22	9.18	509.6	312.3	3.81
	0.8		0.541	4.884	20.74	0.40	3.29	29.25	32.54	93.14	10.46	9.41	505.7	314.7	3.92
	1.2		0.231	2.088	17.69	0.34	2.81	25.04	27.85	105.8	11.89	10.69	491.8	323.6	4.49
5 m ChCl	0.4	26.8	1.032	9.185	22.16	0.44	1.04	9.31	10.35	110.9	12.45	11.19	167.9	947.8	4.95
	0.8		1.070	9.527	21.36	0.42	1.01	9.00	10.01	120.2	13.49	12.13	176.0	904.1	5.73
	1.2		**1.226**	**10.910**	**18.65**	**0.37**	**0.88**	**7.87**	**8.76**	**140.8**	**15.80**	**14.20**	**180.2**	**883.0**	**6.78**
5 m LiTFSI	0.4	13.14	0.054	0.486	24.60	0.48	2.22	19.78	22.00	106.0	11.91	10.71	393.1	404.9	4.36
	0.8		0.026	0.235	23.29	0.45	2.11	18.74	20.85	109.5	12.31	11.06	384.9	413.5	4.73
	1.2		**0.518**	**4.679**	**21.65**	**0.42**	**1.97**	**17.50**	**19.46**	**119.2**	**13.39**	**12.04**	**390.9**	**407.1**	**5.33**
10 m ChCl	0.4	9.79	0.518	4.607	16.14	0.32	1.01	8.96	9.97	100.8	11.31	10.17	179.3	887.6	4.25
	0.8		0.506	4.501	16.52	0.32	1.03	9.15	10.18	102.9	11.55	10.38	187.0	851.1	4.61
	1.2		0.583	5.192	14.32	0.28	0.89	7.97	8.87	117.7	13.21	11.88	186.3	854.4	5.32
10 m LiTFSI	0.4	4.79	0.222	2.010	18.37	0.36	2.38	21.16	23.53	90.90	10.21	9.18	392.0	406.0	4.14
	0.8		0.227	2.051	18.00	0.35	2.31	20.61	22.92	88.32	9.92	8.92	371.0	429.0	4.05
	1.2		0.264	2.388	15.46	0.30	1.99	17.75	19.74	92.33	10.37	9.32	334.0	476.5	4.27
15 m ChCl	0.4	4.35	0.123	1.095	30.15	0.59	2.26	20.16	22.43	112.9	12.67	11.39	448.2	355.1	5.19
	0.8		0.125	1.109	29.76	0.58	2.22	19.81	22.03	113.1	12.70	11.41	441.4	360.6	5.25
	1.2		0.127	1.134	29.10	0.57	2.14	19.09	21.23	111.4	12.50	11.24	418.6	380.2	5.14
15 m LiTFSI	0.4	1.55	0.071	0.637	18.77	0.36	4.90	43.61	48.50	105.1	11.81	10.62	959.9	18.77	4.76
	0.8		0.073	0.655	18.25	0.35	4.76	42.36	47.11	104.8	11.78	10.59	929.6	18.25	4.61
	1.2		0.079	0.715	16.72	0.32	4.35	38.76	43.11	112.5	12.64	11.36	913.1	16.72	4.94
20 m ChCl	0.4	2.56	0.077	0.681	28.55	0.56	3.43	30.53	33.96	118.5	13.30	11.96	654.4	243.2	5.04
	0.8		0.076	0.675	28.80	0.57	3.46	30.84	34.30	114.9	12.89	11.59	640.5	248.5	4.96
	1.2		**0.094**	**0.836**	**23.26**	**0.46**	**2.79**	**24.86**	**27.65**	**136.5**	**15.32**	**13.77**	**613.3**	**259.5**	**5.89**
20 m LiTFSI	0.4	0.71	0.042	0.377	14.52	0.28	6.37	56.72	63.09	111.4	12.52	11.26	1295.0	122.9	4.68
	0.8		0.036	0.325	16.81	0.33	7.32	65.19	72.50	106.3	11.94	10.74	1419.8	112.1	4.45
	1.2		**0.037**	**0.331**	**16.53**	**0.32**	**7.16**	**63.76**	**70.91**	**111.9**	**12.57**	**11.30**	**1461.5**	**108.9**	**4.78**

Table S17: Effect of salt concentration and voltages on the ionic conductivity and resistivity of the bulk water-in-salt electrolyte solutions.

Salt conc. (mol·kg^{-1})	**Applied voltage (V)**	**σ in-bulk (mS·cm^{-1})**	**R in-bulk (Ohm·cm)**
1 m ChCl	0.4	54.0	18.52
	0.8	54.1	18.50
	1.2	53.6	18.67
1 m LiTFSI	0.4	29.80	33.6
	0.8	29.62	33.8
	1.2	29.52	33.9
5 m ChCl	0.4	99.5	10.05
	0.8	99.1	10.09
	1.2	99.0	10.10
5 m LiTFSI	0.4	51.98	19.2
	0.8	51.92	19.3
	1.2	51.70	19.34
10 m ChCl	0.4	75.3	13.29
	0.8	75.4	13.26
	1.2	75.1	13.32
10 m LiTFSI	0.4	36.29	27.6
	0.8	36.50	27.4
	1.2	36.40	27.5
15 m ChCl	0.4	62.5	16.01
	0.8	62.8	15.93
	1.2	63.7	15.70
15 m LiTFSI	0.4	17.99	55.60
	0.8	18.00	55.55
	1.2	18.03	55.5
20 m ChCl	0.4	39.07	25.60
	0.8	39.03	25.62
	1.2	39.11	25.57
20 m LiTFSI	0.4	10.69	93.5
	0.8	10.78	92.8
	1.2	10.83	92.3

The quivalent circuit diagram (**Figure S20**) for capacitor cell using LiTFSI electrolyte has been created using the EC-lab software.[13, 14]

Elements of equivalent circuit used: R1+C2/(R2+W2)+C3/R3+C4

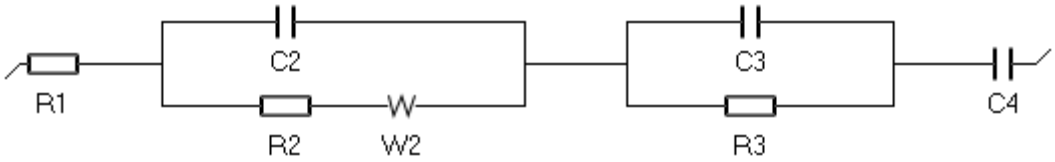

Figure S20: Equivalent circuit model for capacitor using aqueous LiTFSI electrolyte

The possible electrochemical meaning corresponding to different fitting elements has been listed. For example, R1 is equivalent series resistance (ESR), C1 is interfacial contact EDL capacitance, R2 the charge transfer resistance, W2 the Warburg co-efficient, C4 the EDL capacitance within Warburg region, R5 the ion diffusion resistance and C5 is the low frequency EDL capacitance after Warburg region. **Figure S21** shows a good matching of experimental and fitted Nyquist plots of capacitor cells assembled with 1, 5, and 20 mol·kg^{-1} LiTFSI measured at open circuit potential and 1.2 V using above circuit model, thereby demonstrating the appropriateness of the chosen circuit model. The fitting parameters of the circuit model elements are given in **Table S18.**

***Table S18*:** Effect of salt concentration and applied bias potential on different equivalent circuit model elements R1+C2/(R2+W2)+C3/R3+C4. Fitting was carried out at least three times to determine the corresponding standard deviation values.

Circuit elements (unit)	**1 m LiTFSI**		**5 m LiTFSI**		**20 m LiTFSI**	
	OCP	**1.2 V**	**OCP**	**1.2 V**	**OCP**	**1.2 V**
R1 (Ohm)	0.86±0.05	0.80±0.04	0.60±0.03	0.50±0.03	1.85±0.15	1.80±0.14
C2 (F)	6e-5	6e-5	6e-5	6e-5	6e-5	6e-5
R2 (Ohm)	1.40±0.05	1.15±0.04	0.70±0.03	0.50±0.03	1.40±0.12	1.10±0.11
W2 (Ohm.s^-1/2)	3.02±0.15	2.85±0.12	1.10±0.06	0.90±0.05	3.20±0.16	2.95±0.14
C3 (F)	0.05	0.05	0.06	0.06	0.045	0.035
R3 (Ohm)	0.20±0.05	0.15±0.05	0.12±0.05	0.11±0.05	1.00±0.05	0.80±0.05
C4 (F)	0.13±0.02	0.15±0.02	0.14±0.02	0.16±0.02	0.12±0.03	0.10±0.03

Expectedly, the influence of salt concentrations and cell voltages on different resistances is in line with different extracted resistances (ESR, CTR, IDR, and EDR) as shown in the main manuscript **Figure 4a**, **Figure 4b**, and *supporting information* **Table S10** and **Table S15**. Likewise, the values of EDL capacitance are in agreement with **Figure 4c**, **Table S11, Table S12** and **Table S16**. Besides, the trend of Warburg co-efficient W2 values are also in harmony with the in-pore diffusivity and ion transport resistance as outlined in **Figure 5b** and **Figure 5c**, **Table S12** and **Table S16**.

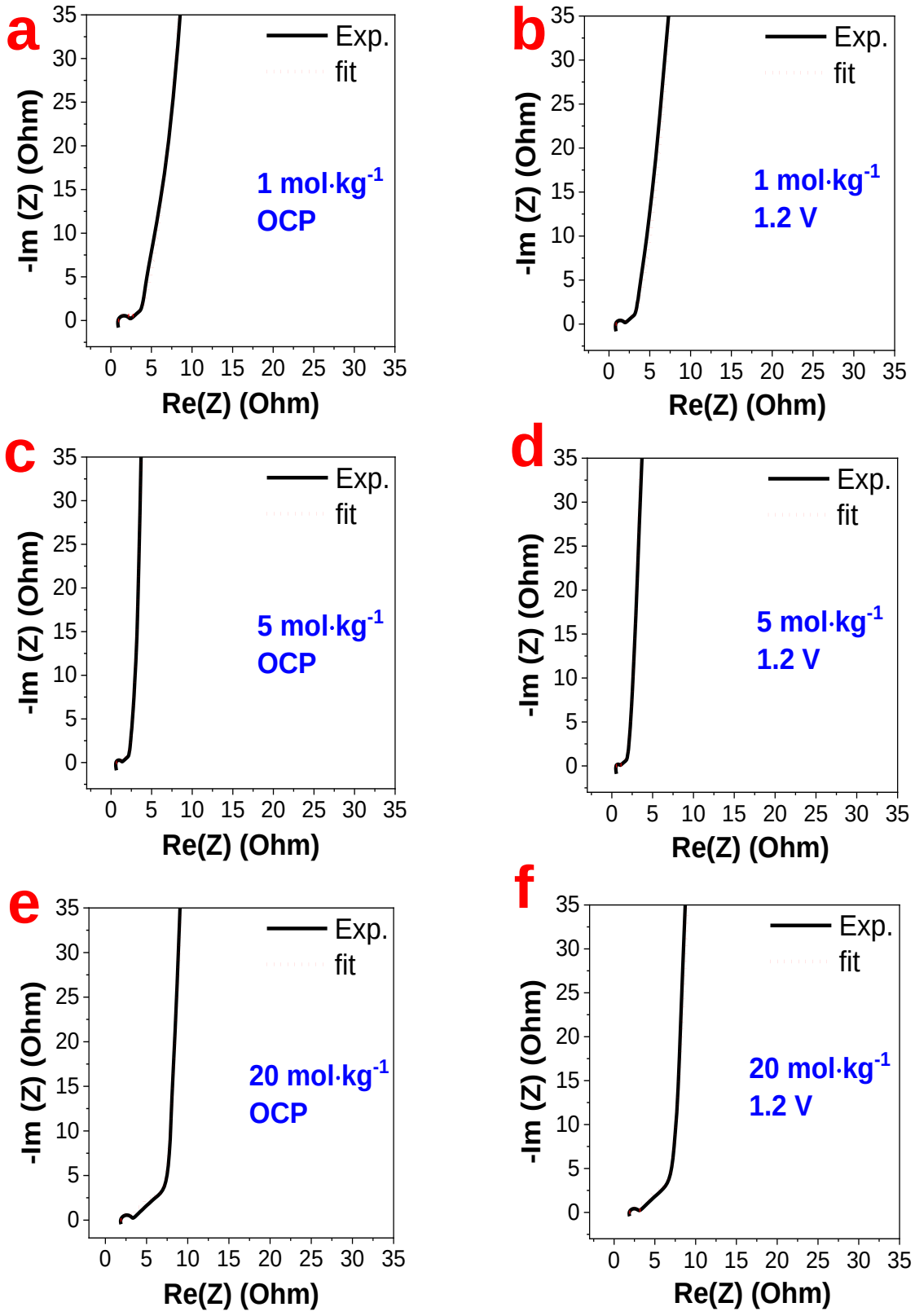

***Figure S21*:** The experimental and fitted Nyquist plot of capacitor cell assembled with 1, 5, and 20 mol·kg^{-1} LiTFSI measured at open circuit potential (a, c, e) and 1.2 V (b, d, f).

References

1. K. Tanaka, M. Nomura, J. Chem. Soc., Faraday Trans., 1987, 83, 1779-1782.

2. Q. Abbas, P. Nürnberg, R. Ricco, F. Carraro, B. Gollas, M. Schönhoff., Adv. Energy Sustainability Res., 2021, 2, 2100115.

3. M. Chintapalli, K. Timachova, K.R. Olson, S. J. Mecham, D. Devaux, J.M. Desimone, N.P. Balsara., Macromolecules., 2016, 49, 3508–3515.

4. M. Gouverneur, J. Kopp, L. Van Wüllen, M. Schönhoff, Phys. Chem. Chem. Phys., 2015, 17, 30680–30686.

5. K. Chai, X. Lu, Y. Zhou, H. Liu, G. Wang, Z. Jing, F. Zhu, L. Han, J Mol Liq., 2022, 362, 119742

6. S. Elderderi, L. Wils, C. Leman-Loubière, S. Henry, H.J. Byrne, I. Chourpa, E. Munnier, A.A. Elbashir, L. Boudesocque-Delaye, & Franck Bonnier, Anal. Bioanal. Chem., 413.19 (2021): 4785-4799.

7. S. Krachkovskiy, M. Dontigny, S. Rochon, C. Kim, M.L. Trudeau, K. Zaghib, J. Phys. Chem. C., 2020, 124, 24624–24630.

8. P. Ahuja, V. Sahu, S.K. Ujjain, R.K. Sharma, G. Singh, Electrochim Acta., 2014, 146, 429–436.

9. K.L. Van Aken, J.K. McDonough, S. Li, G. Feng, S.M. Chathoth, E. Mamontov, P.F. Fulvio, P.T. Cummings, S. Dai, Y. Gogotsi, J. Phys. Condens. Matter., 2014, 26, 284104.

10. R.D. Armstrong, J Electroanal Chem., 1986, 198, 177-180.

11. L. Borchardt, D. Leistenschneider, J. Haase, M. Dvoyashkin, Adv Energy Mater., 2018, 8 1800892.

12. A.C. Forse, J.M. Griffin, C. Merlet, J. Carretero-Gonzalez, A.R.O. Raji, N.M. Trease, C.P. Grey, Nat Energy., 2017, 2, 16216.

13. C. Lei, F. Markoulidis, Z. Ashitaka & C. Lekakou, Electrochimica acta., 2013, 92, 183-187.

14. B. A. Mei, O. Munteshari, J. Lau, B. Dunn, & L. Pilon., J. Phys. Chem. C., 2018, 122, 194−206